Joint Inversion of Gravity Gradiometry Data by Model-Weighted Clustering in Logarithmic Space

Zhengwei Xu, Rock Physics Lab, University of Houston; Le Wan, Muran Han and Michael S. Zhdanov, University of Utah; Yue Mao, Colorado School of Mines.*

SUMMARY

This paper develops a method of joint inversion of the different individual components of full-tensor gradient (FTG) data using the re-weighted regularized Newton-Gauss algorithm based on the clustering method. The clustering technique is used to enforce the density to be distributed around the specific a priori values determined from either petrophysical data or the rock sample measurement. To keep the density of the inverse model within the imposed boundaries, we implemented the inversion algorithm in the logarithmic model space. In addition, we applied the model weighting matrix to the clustering functional in order to guarantee the robustness of the inversion. Compared with a standard smooth density inversion, the new inversion approach predicts accurately the values of the density, and also improves the spatial resolution of the anomalous bodies, which is important in studying the complex geological structures. We present a model study and a case study for the new inversion approach using FTG gravity gradiometry data from Nordkapp Basin, Barents Sea.

INTRODUCTION

The emergence and successful development of full tensor gravity gradiometry (FTG), made it possible to use FTG data to improve the effectiveness of the gravity method in mineral and hydrocarbon (HC) exploration (Zhdanov et al., 2009). For example, salt diapirs, as a kind of typical geological structure, are bounded within the host rock by a sharp boundary.

The traditional regularization algorithms are based on applying the maximum smoothness (Constable, et al., 1987) and minimum norm (Bell et al., 1977) constraint to the inverse model. But it fails to recognize the sharp boundaries of geological formations (Zhdanov, 2002, 2015). Portniaguine and Zhdanov (1999) introduced a concept of focusing inversion based on the minimum support or minimum gradient support constraints which provide the inverse models with sharp boundaries. Another approach is based on application of the joint inversion by integrating multiple datasets to mitigate some of inherent ambiguity t (e. g., Vozoff and Jupp, 2007; Coutant et al., 2012; Zhdanov and Cox, 2013; Kamm et al., 2015; Xu and Zhdanov, 2015).

In order to exploit anomalous targets with high contrasts by given a priori geologic information, an approach based on binary transforms was initially developed by transforming the continous function into the binary function (Zhdanov and Cox, 2013). Zhdanov and Lin (2017) extended the approach from binary to quasi-multinary transforms. Nevertheless, in order to migitate the difficulty in implementing the derivative-based minimization of the Tikhonov parametric functional, it is necessary to transform the continuous functions of the model parameters and their sensitvities to their multinary function.

As an alternative approach in producing a focusing image without multinary transform, Sun and Li (2015, 2016a, and 2016b) proposed a multi-domain joint using the guided fuzzy *c*-means (FCM) clustering method to manage to solve the multimodal inverse problem. But the FCM clustering objective functional fails to take weighting matrices for the model parameters into calculation, of which the function is to ensure observed data are of equal snensitivity to the model-weighted parameters.

To overcome the two main shortcomings of the current focusing-based approaches, in this paper, we apply a deterministic approach to minimization of the classic Tikhonov regularization parametric functional with the model-weighted FCM clustering objective functional. In order to make the convergence fast, the Newton-Gauss algorithm is implemented in the weighted model space to invert density distribution by jointly using the different individual components of the FTG tensor. Furthermore, in a similar manner as it was done in the framework of multinary inversion, we also transfer the original model parameters into logarithmic space to guarantee that the corresponding parameters will always be found within the imposed boundaries.. The approach is tested through 3D synthetic study and a case study, of which a field FTG gravity gradiometry data acquired in the Nordkapp Basin of the Barents Sea.

WEIGHTED FCM INVERSION METHODOLOGY

Consider forward geophysical problems for multiple geophysical data sets. These problems can be described by the operator relationships:

$$\boldsymbol{d}^{(i)} = \widehat{\boldsymbol{A}}^{(i)}(\widehat{\boldsymbol{m}}) = \boldsymbol{A}^{(i)}(\boldsymbol{m}), i = 1,2,3,\dots,N; \qquad (1)$$

10.1190/segam2019-3214793.1

where, in a general case, $\hat{\boldsymbol{m}}$ stands for the unknown sets of model parameters in logarithmic space to make sure original model $\boldsymbol{m}$ will always within the imposed and reasonable boundary as:

$$\hat{\boldsymbol{m}} = ln\frac{\boldsymbol{m}-\boldsymbol{m}^-}{\boldsymbol{m}^+-\boldsymbol{m}}, \qquad (2)$$

and $\hat{\boldsymbol{A}}^{(i)}$ is corresponding a linear or nonlinear operator in logarithmic space. $\boldsymbol{d}^{(i)}$ $(i = 1,2,3,\dots,n)$ are different observed data sets which are sensitive to different physical properties but are collected over the same survey area.

The joint inversion recovers density property by using a single parametric functional to the following formula:

$$\boldsymbol{P}^{\alpha}(\hat{\boldsymbol{m}}) = \sum_{i=1}^{N} \boldsymbol{\varphi}_w^{(i)}(\hat{\boldsymbol{m}}) + \alpha \boldsymbol{S}_{\boldsymbol{w}}(\hat{\boldsymbol{m}}) + \lambda \boldsymbol{\Phi}_{w\_fcm}(\hat{\boldsymbol{m}}) \qquad (3)$$

where α and λ are the regularization and compactness parameter, respectively. The $\boldsymbol{\varphi}_w^{(i)}(\hat{\boldsymbol{m}})$ is the data-weighted misfit functional between the predicted data $\hat{\boldsymbol{A}}^{(i)}(\hat{\boldsymbol{m}})$, and the observed data $\boldsymbol{d}^{(i)}$ for one specific dataset i:

$$\boldsymbol{\varphi}_w^{(i)}(\hat{\boldsymbol{m}}) = \left\| \widehat{\boldsymbol{W}}_d^{(i)} \hat{\boldsymbol{A}}^{(i)}(\hat{\boldsymbol{m}}) - \widehat{\boldsymbol{W}}_d^{(i)} \boldsymbol{d}^{(i)} \right\|_{L_2}^2 \qquad (4)$$

and the $\boldsymbol{S}_{\boldsymbol{w}}(\hat{\boldsymbol{m}})$ is the model-weighted stabilizing functional that is usually introduced as the least-squares difference between the regularized solution and some a priori model, $\hat{\boldsymbol{m}}_{\boldsymbol{apr}}$ as:

$$\boldsymbol{S}_{\boldsymbol{w}}(\hat{\boldsymbol{m}}) = \left\| \widehat{\boldsymbol{W}}_{\boldsymbol{m}} \hat{\boldsymbol{m}} - \widehat{\boldsymbol{W}}_{\boldsymbol{m}} \hat{\boldsymbol{m}}_{\boldsymbol{apr}} \right\|_{L_2}^2 \qquad (5)$$

where $\widehat{\boldsymbol{W}}_{\boldsymbol{d}}$ and $\widehat{\boldsymbol{W}}_{\boldsymbol{m}}$ are the data the data and model weighting matrices, respectively. Eventually, we conduct the FCM objective functional term $\boldsymbol{\Phi}_{w\_fcm}(\hat{\boldsymbol{m}})$ as sum of two terms, one is least-squares difference between weighted model parameters $\widehat{\boldsymbol{mw}} = \widehat{\boldsymbol{W}}_{\boldsymbol{m}} \hat{\boldsymbol{m}}$ and average physical property value (center) $\widehat{\boldsymbol{Vw}}_{\boldsymbol{k}} = \widehat{\boldsymbol{W}}_{\boldsymbol{m}} \hat{\boldsymbol{V}}_{\boldsymbol{k}},$ for the kth petrophysical unit. Another is to guide weighted $\widehat{\boldsymbol{Vw}}_{\boldsymbol{k}}$ toward to the target cluster center $\widehat{\boldsymbol{Tw}}_{\boldsymbol{k}} = \widehat{\boldsymbol{W}}_{\boldsymbol{m}} \hat{\boldsymbol{T}}_{\boldsymbol{k}}$(Sun & Li 2015a):

$$\boldsymbol{\Phi}_{w\_fcm}\left(\hat{\boldsymbol{m}}; \hat{\boldsymbol{U}}_{\boldsymbol{k}}^{\boldsymbol{q}}, \widehat{\boldsymbol{Vw}}_{\boldsymbol{k}}\right) = \sum_{k=1}^{C} \left(\hat{\boldsymbol{m}} - \hat{\boldsymbol{V}}_k\right)^T \widehat{\boldsymbol{W}}_{\boldsymbol{m}}^{\ T} \widehat{\boldsymbol{W}}_{\boldsymbol{m}} \boldsymbol{U}_k^q \left(\hat{\boldsymbol{m}} - \hat{\boldsymbol{V}}_k\right) + \sum_{k=1}^{C} \eta_k \left\| \widehat{\boldsymbol{W}}_{\boldsymbol{m}} \hat{\boldsymbol{V}}_k - \widehat{\boldsymbol{W}}_{\boldsymbol{m}} \hat{\boldsymbol{T}}_k \right\|_{L_2}^2 \qquad (6)$$

where η_k stands for closeness parameters and $\boldsymbol{U}_k$ is the membership value in which each element can be interpreted as the probability of the corresponding model cell belonging to the kth petrophysical unit. (Sun & Li 2017). One of the advantages of selecting appropriate model weighting coefficients is to eliminate the effect of the units and magnitudes. Comparing with traditional model weighting approach, as the square root of the integrated sensitivity matrix, a modified model weighting matrix, in this paper, should be selected:

$$\widehat{\boldsymbol{W}}_{\boldsymbol{m}} = diag \sqrt[4]{\left(\frac{\hat{\boldsymbol{F}}_{\boldsymbol{m}_n}^{(i)}}{max\left(\hat{\boldsymbol{F}}_{\boldsymbol{m}_n}^{(i)}\right)}\right)^T \cdot \left(\frac{\hat{\boldsymbol{F}}_{\boldsymbol{m}_n}^{(i)}}{\max\left(\hat{\boldsymbol{F}}_{\boldsymbol{m}_n}^{(i)}\right)}\right)} \qquad (7)$$

where $\hat{\boldsymbol{F}}_{\boldsymbol{m}_n}^{(i)}$ is the Fr é chet derivative in the space of logarithmic model parameters as of the forward operator $\hat{\boldsymbol{A}}^{(i)}$. This choice of model weighting matrix ensures a uniform sensitivity to the different model parameters (Nocedal *et al.* 1999). For gravity survey, the linear Fréchet derivative operator in log space can be represented as the original forward modeling operator $\boldsymbol{A}^{(i)}$ by derivative of original model parameter $\boldsymbol{m}$ with respective with logarithmic model parameter $\hat{\boldsymbol{m}}$, shown in Eq. (2) as:

$$\hat{\boldsymbol{F}}_{\boldsymbol{m}_n}^{(i)} = \boldsymbol{A}^{(i)} \cdot \frac{\boldsymbol{m}^+ - \boldsymbol{m}^-}{\left(1+exp(\hat{\boldsymbol{m}})\right)^2} \cdot exp(\hat{\boldsymbol{m}}) \qquad (8)$$

and $\widehat{\boldsymbol{W}}_{\boldsymbol{m}}$is updated for each iteration as $\hat{\boldsymbol{m}}$ update, so-called re-weighted.

Substituting Eq. (6) into Eq. (3), we find:

$$\boldsymbol{P}^{\alpha,\lambda}\left(\hat{\boldsymbol{m}}; \hat{\boldsymbol{U}}_{\boldsymbol{k}}^{\boldsymbol{q}}, \widehat{\boldsymbol{Vw}}_{\boldsymbol{k}}\right) = \sum_{i=1}^{N} \boldsymbol{\varphi}_{\boldsymbol{w}}^{(i)}(\hat{\boldsymbol{m}}) + \boldsymbol{\alpha} \boldsymbol{S}_{\boldsymbol{w}}(\hat{\boldsymbol{m}}) + \boldsymbol{\lambda} \boldsymbol{\Phi}_{\boldsymbol{w\_fcm}}(\hat{\boldsymbol{m}}) \qquad (9)$$

In this paper, there are two key points to apply model parameter weighting on the FCM objective functional. First of all, for physical point of view, the linear operator $\boldsymbol{A}^{(i)}$ acts from the space M to the space D. It is easier to solve the inverse problem if the corresponding operator equation describes the transformation within the same vector space, for example, within a space of the model parameters M. On the other hand, it can be shown that, by reformulating the minimization problem in Eq. (9) using a space of weighted parameters, the iterative process converges faster than the one in a space of original model parameters (Zhdanov, 2002).

According to the basic principles of the regularization method, we have to find a model, $\hat{\boldsymbol{m}}$, a quasi-solution of the inverse problem, that minimizes the parametric functional:

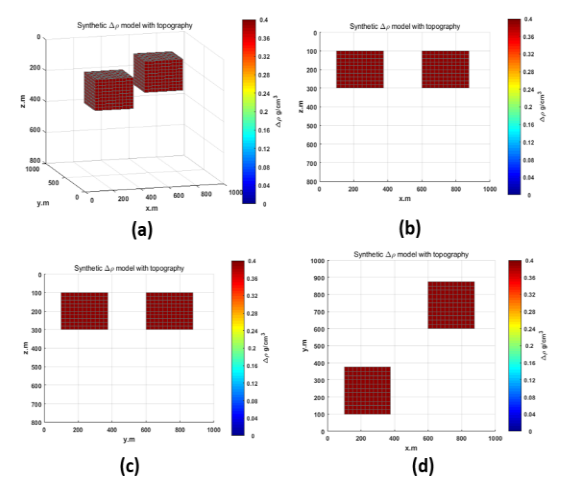

Fig. 1. The true synthetic model (a). 3D view of the model. (b). X-Z section view of the model, (c), Y-Z section view of the model, (d) X-Y plane view of the model.

10.1190/segam2019-3214793.1

$$\boldsymbol{P}^{\alpha}\left(\widehat{\boldsymbol{m}}, \boldsymbol{U}_k^{(i)}, \boldsymbol{V}_k^{(i)}, d\right) = min \qquad (11)$$

SYNTHETIC STUDY: TWO-BODIES MODEL

In our model study, two density models which consist of two rectangular bodies with same sizes are used, densities and burial depths submerged in a 0 g/cm^3 homogenous background (Figure. 1). The two of the bodies are both located at a depth of 100 m. The body sides in the x, y, and z directions have a length of 150 m, 150 m, and 200 m, respectively. The two bodies with positive anomalous densities of 0.4 g/cm^3. The partial synthetic FTG data for this model were denoted as g_{zz}, g_{xz}, and g_{yz}. In order to improve the effectiveness of the new algorithm, both traditional regularization inversion with and without FCM term are carried out. The iterative process of the RCG algorithm was terminated when the norm of the difference between the observed and predicted data reached the level of noise, 3%.

Figure. 2 and 3 show the traditional regularization inversion results without and with considering FCM term, respectively. It demonstrates that the proposed inversion technology is not only able to covert the value of density, but also improve the spatial imaging of anomaly bodies, even more sharp than the traditional one.

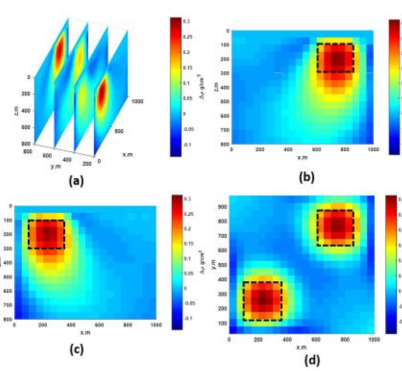

Fig. 2. The inversion results without considering FCM (a). 3D slice view of the model. (b). X-Z section view of the model (Y = 800 m), (c), X-Z section view of the model (Y=200 m), (d) X-Y plane view of the model (Z = 200 m).

Additionally, the recovered value of density is about 0.3 g/cm^3 which is still far away from the assigned 0.4 g/cm^3 However, the proposed method is able to reach accurate values of the anomaly bodies and significantly improves the image, especially stand out the clear boundaries of the anomaly bodies.

The Figure. 4 shows comparison of the histograms of traditional regularization and the one with FCM, it indicates

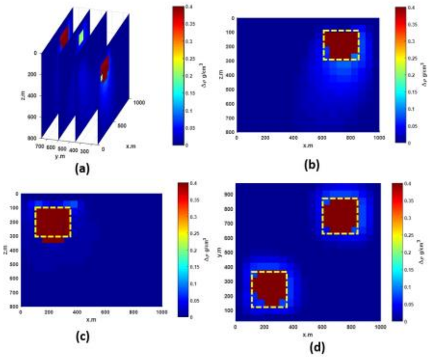

Fig. 3. The inversion results considering FCM (a). 3D view of the model. (b). X-Z section view of the model, (c), X-Z section view of the model, (d) X-Y plane view of the model.

that an inversion for the a priori petrophysical data achievable. In another word, a model whose cell values adequately reproduce the statistical behavior of the true model cell values is produced.

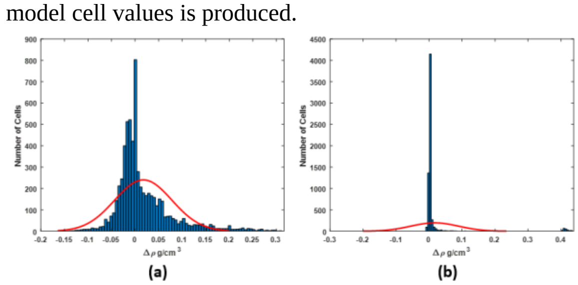

Fig. 4. (a) The distribution of the inverted density values without considering FCM. (b). Histogram of inverted density values with considering FCM.

CASE STUDY: INVERISON OF FTG DATA AT THE NORDKAPP BASIN

The FTG survey was conducted within the Nordkapp basin in the Barents Sea, offshore Norway (Figure 5.a). The southwestern part sub-basin (Obelix survey location)

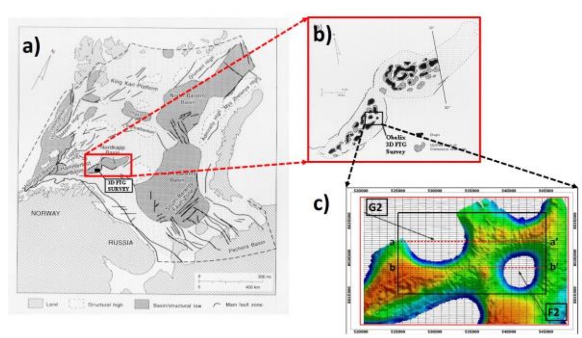

Fig. 5. The true synthetic model (a). 3D view of the model. (b). X-Z section view of the model, (c), Y-Z section view of the model, (d) X-Y plane view of the model.

10.1190/segam2019-3214793.1

contains some 17 salt diapirs located along the basin's axis (Figure 5.b). The purpose of the FTG survey was to obtain additional information for evaluation of the salt diapirs G2 and F2 (Figure 5.c) overhang geometries.

A typical density of the base tertiary rocks in the area of investigation is within 2.30-2.38 g/cm^3. The salt diapirs, of which density is estimated as 2.1-2.15 g/cm^3, are often visualized by negative density anomalies. The density of the rocks of the deeper basement is approximately 2.5-2.54 g/cm^3. Therefore, three clusters corresponding three different geologic units of which the centers are -0.2 g/cm^3, 0 g/cm^3, and 0.2 $g/cm^3$are established. We have applied the FCM clustering inversion to combine the two components of the gravity tensor: g_{zz}, and g_{yz}. A modeling domain with 20 km (east-west, x-axis) × 11 km (north-south, y-axis) and extended at a depth of about 8 km is selected.

Figure 6.a and b illustrate the joint inversion results for the g_{zz} and g_{yz} components in the form of vertical sections along the profiles a-a' and b-b'. The horizontal section (z=3000 m) is shown in Figure 6.c. One can clearly see the salt diapirs G2 and F2 geometry and the boundary between salt diapirs and host rock. The histograms shown in Figure 6.d indicates three clear geologic units representing the corresponding anomalous density values of salt diapir, host rock, and basement rock, respectively and that the possible density values are around -0.2, 0, and 0.2 g/cm^3.

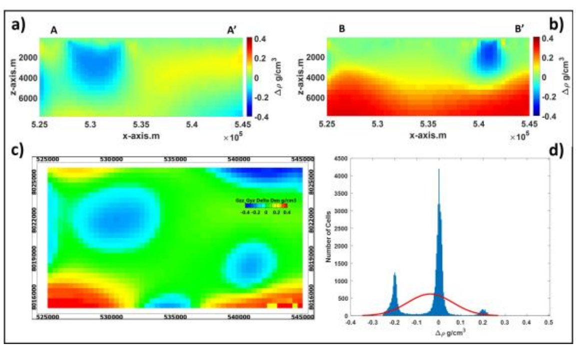

Fig. 6. The true synthetic model (a). 3D view of the model. (b). X-Z section view of the model, (c), Y-Z section view of the model, (d) X-Y plane view of the model.

Figure 7 shows a 3D image of the results of the joint inversion of three components of the gravity tensor: g_{zz} and g_{yz}. It shows that in this image the domains haves an anomalous density less than -0.1 g/cm^3. It also shows that the two salt diapirs G2 and F2 geometry is consistent with the seismic interpretation as well.

CONCLUSIONS

In this paper, we have developed a new algorithm and a computer code for inversion of the FTG data, which takes

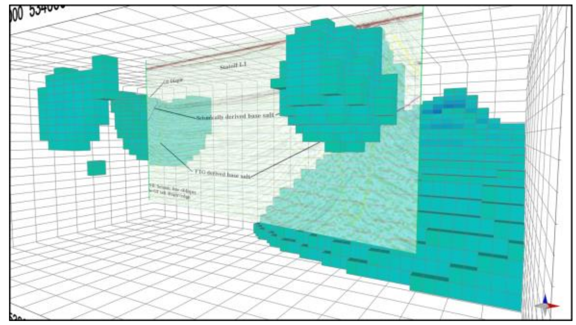

Fig. 7. The true synthetic model (a). 3D view of the model. (b). X-Z section view of the model, (c), Y-Z section view of the model, (d) X-Y plane view of the model.

into account the known geological information about the subsurface density values. To ensure a stable convergence, we use a regularized Newton-Gauss method in the weighted model parameter space. In addition, a logarithmic model parameter was used to guarantee the solution being constrained within the imposed boundaries. Finally, a model-weighted FCM clustering functional was introduced to make the inversion stable and reliable.

The synthetic inversion results demonstrate that the new inversion technology produces the correct values of the density, and also improves the spatial resolution of anomalous bodies, recovering the sharp boundaries correctly. We have applied the developed method to interpretation of the FTG survey data collected in the Barents sea. It is clear that the marine FTG survey is very sensitive to the density distribution in geological formations. The gravity tensor components represent well the density anomalies associated with complex salt diapirs and their related structural traps.

The 3D inversion with FCM clustering of FTG data made it possible to resolve the complex geological structures of the salt formations. We have run inversion of the individual components of the full gravity gradient tensor, and we have also applied a joint inversion. The numerical results demonstrated that the joint inversion with FCM clustering functional helped sharpening the inverse image and producing a reliable 3D model of the density distribution in the area of FTG survey.

ACKNOWLEDEMENT

We are thankful to the Rock Physics Lab, University of Houston and to the Consortium for Electromagnetic Modeling and Inversion, University of Utah for supporting the research.

We are thankful to Dr. Brian Farrelly for providing the FTG data.

The authors also thanks to Dr. Jiajia Sun and Mr. Huw James for providing invaluable feedback and many constructive discussion and suggestions.

REFERENCES

Bell, J. B., A. N. Tikhonov, and V. Y. Arsenin, 1978, Solutions of Ill-posed problems: Mathematics of Computation, **32**, 1320, doi: https://doi.org/10.2307/2006360.

Constable, S. C., R. L. Parker, and C. G. Constable, 1987, Occam's inversion: A practical algorithm for generating smooth models from electromagnetic sounding data: Geophysics, **52**, 289–300, doi: https://doi.org/10.1190/1.1442303.

Coutant, O., M. L. Bernard, F. Beauducel, F. Nicollin, M. P. Bouin, and S. Roussel, 2012, Joint inversion of P-wave velocity and density, application to La Soufrière of Guadeloupe hydrothermal system: Geophysical Journal International, **191**, 223-742, doi: https://doi.org/10.1111/j.1365-246x.2012.05644.x.

Kamm, J., I. A. Lundin, M. Bastani, M. Sadeghi, L. B. Pedersen, 2015, Joint inversion of gravity, magnetic, and petrophysical data—A case study from a gabbro intrusion in Boden, Sweden: Geophysics: **80**, no. 5, B131-B152, doi: https://doi.org/10.1190/geo2014-0122.1.

Portniaguine, O., and M. S. Zhdanov, 1999, Focusing geophysical inversion images: Geophysical, **64**, 874–887, doi: https://doi.org/10.1190/1.1444596.

Sun, J., and Y. Li, 2015, Multidomain petrophysically constrained inversion and geology differentiation using guided fuzzy c-means clustering: Geophysics, **80**, no. 4, ID1-ID18, doi: https://doi.org/10.1190/geo2014-0049.1.

Sun, J., and Y. Li, 2016, Joint inversion of multiple geophysical and petrophysical data using generalized fuzzy clustering algorithms: Geophysical Journal International, **208**, no. 2, 1201–1216, doi: https://doi.org/10.1093/gji/ggw442.

Vozoff, K., and D. L. B. Jupp, 2007. Joint inversion of geophysical data: Geophysical Journal International, **42**, 977–991, doi: https://doi.org/10.1111/j.1365-246x.1975.tb06462.x.

Xu, Z., and M. S. Zhdanov, 2015, Three-dimensional Cole-Cole model inversion of induced polarization data based on regularized conjugate gradient method: IEEE Geoscience and Remote Sensing Letters, **12**, DV81-D94, doi: https://doi.org/10.1109/lgrs.2014.2387197.

Zhdanov, M. S., 2002. Geophysical inverse theory and regularization problems: Elsevier.

Zhdanov, M. S., 2009. New advances in regularized inversion of gravity and electromagnetic data: Geophysical Prospecting, **57**, 463–478, doi: https://doi.org/10.1111/j.1365-2478.2008.00763.x.

Zhdanov, M. S., 2015. Inverse theory and applications in geophysics, **vol. 36**: Elsevier.

Zhdanov, M. S. and L. H. Cox, 2013. Multinary inversion for tunnel detection: IEEE Geoscience and Remote Sensing Letters, **10**, 1100–1103, doi: https://doi.org/10.1109/lgrs.2012.2230433.

Zhdanov, M. S. and W. Lin, 2017. Adaptive multinary inversion of gravity and gravity gradiometry data adaptive multinary inversion of gravity data: Geophysics, **82**, no. 6, G101–G114, doi: https://doi.org/10.1190/geo2016-0451.1.